Robust GPS-Based Timing for Phasor Measurement Units: A Position-Information-Aided Approach

Daniel Chou, Liang Heng, and Grace XingXin Gao,
University of Illinois Urbana-Champaign

BIOGRAPHIES

Daniel Chou is a graduate student in the Department of Electrical and Computer Engineering, University of Illinois at Urbana-Champaign. He received his B.S. in Electrical Engineering from Arizona State University in 2013. His current research projects include designing and implementing countermeasures against malicious attacks on civilian grade GPS receivers utilized in phasor measurement units.

Liang Heng is a postdoctoral research associate in the Department of Aerospace Engineering, University of Illinois at Urbana-Champaign. He received the B.S. and M.S. degrees from Tsinghua University, China in 2006 and 2008, and the Ph.D. degree from Stanford University in 2012, each in Electrical Engineering. His research interests are cooperative navigation and satellite navigation. He is a member of the Institute of Electrical and Electronics Engineer (IEEE) and the Institute of Navigation (ION).

Grace Xingxin Gao is an assistant professor in the Aerospace Engineering Department at University of Illinois at Urbana-Champaign. She received her B.S. degree in Mechanical Engineering in 2001 and her M.S. degree in Electrical Engineering in 2003, both at Tsinghua University, China. She obtained her Ph.D. degree in Electrical Engineering at Stanford University in 2008. Before joining Illinois at Urbana-Champaign as an assistant professor in 2012, Prof. Gao was a research associate at Stanford University. Professor Gao has won a number of awards, including RTCA William E. Jackson Award, Institute of Navigation Early Achievement Award, 50 GNSS Leaders to Watch by GPS World Magazine, and multiple best presentation awards at ION GNSS conferences.

ABSTRACT

The security and reliability of GPS receivers are critical to Phasor Measurement Units (PMUs). These devices provide synchronized voltage and current phasor measurements in power systems based on GPS timing. However, due to the unencrypted nature and low received signal to noise ratio of civil GPS signals, jamming and spoofing attacks on GPS receivers can pose a risk to both the position and timing solutions.

In this work, we aim for robust GPS time transfer for PMUs. We achieve this goal by taking advantage of the static nature of PMUs. We propose a position-information-aided vector tracking loop to improve tracking capabilities and ensure continued operation through various attacks. To evaluate the effectiveness of the algorithm presented in this paper, we further conduct field experiments. Our test shows that the proposed position-information-aided vector tracking approach 1) improves the robustness of GPS receivers used in PMUs against jamming; 2) is able to successfully detect record-and-reply attacks; and 3) improves the accuracy of timing solutions.

INTRODUCTION

Invented in the 1980s, Phasor Measurement Units (PMU), also known as synchrophasors, are GPS based devices that provide precise and synchronous electrical wave measurements at frequencies up to 60 Hz. The high speed measurements generated by PMUs are capable of providing the state estimators with information at subsecond time frames, allowing dynamic state measurements of the power system. Additionally, since PMUs across the country use the GPS system as a common time source, the phasor measurements collected by individual units can be placed onto the same phasor diagram without regard to distance or transmission times. This information allows for fine-tuning of the power system that was previously unattainable using the SCADA system. The near real-time measurements collected by PMUs would allow for adaptive and robust state adjustments to account for any changes in the system. Figure 1 illustrates the difference between measurements collected by SCADA and a PMU during disturbance in a power grid in Oklahoma [1].

GPS vulnerabilities affect PMUs

PMUs are vulnerable to interference and spoofing attacks due to their dependence on GPS. The U.S. Energy Information Administration (E.I.A.) is considering implementing a system where the measurements from the PMU network is used to automatically balance the energy

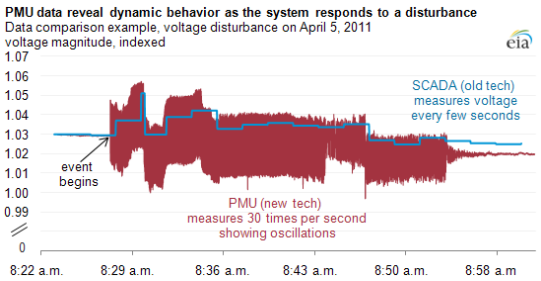

Figure 1: Disturbance in the power grid: SCADA and PMU comparison [1].

distribution in the power grid. While doing so would improve the efficiency and robustness of the power system, the security and stability of the power system is of the utmost importance. The security risks introduced by using GPS-based devices prevents PMUs from being fully integrated into the power system. The risks include vulnerability to jamming and spoofing attacks.

Due to the weak signal strength and unencrypted nature of the civil GPS signals, interference and attacks on a GPS receiver can potentially alter both position and time solutions generated by the receivers. There are intentional and unintentional attack, such as jamming [2,3], spoofing [4-6], and interference due to high powered radio signals bleeding through from nearby frequency bands and naturally occurring electromagnetic fields [7,8].

Our approach: position-information-aided (P.I.A.) vector tracking

Our approach of P.I.A. tracking loop aims to utilize the static nature of the GPS receivers used in PMUs to enhance tracking performance. The concept was introduced by [9]. By leveraging the knowledge of the true position of GPS receivers used in PMUs, we can accurately predict the code and carrier measurements by projecting the relative position and velocity between satellites and the receiver on the line-of-sight (LOS) direction. This type of receiver architecture is referred to as "vector tracking" and has been shown to increase immunity to interference and jamming. Vector tracking combines signal tracking and position/velocity estimation into one algorithm, allowing information from one channel to aid in the tracking of another. The main downside to vector tracking is the high computation time required, however for the purposes of this work processing power is not of major concern.

Tracking robustness can also be improved through the use of Kalman filtering and since the receivers in a PMU must remain static, the parameters of the tracking loops can be adaptively chosen to narrow the loop filter bandwidth. The narrowband tracking loop limits receiver noise which reduces the effective radius of any jamming attacks.

Additionally, the P.I.A vector tracking approach allows for a natural defense against meaconing attacks. Meaconing signals are simply authentic GPS signals being recorded somewhere else and then rebroadcasted. Since the P.I.A. vector tracking approach is dependent on the true position of the GPS receiver, then the proposed tracking loop will fail to function in the case of a meaconing attack, therefore being able to detect meaconing.

Our testbed

To fully understand the real-life impacts of a spoofed or jammed GPS signal on the PMU, and by extension the power grid, we must be able to test its effects in a controlled environment. At the University of Illinois Urbana-Champaign, the Trustworthy Cyber Infrastructure for the Power Grid (TCIPG) has built a testbed specifically for emulating large-scale power systems using high-end simulation equipment. The testbed currently contains ~10 PMUs, two are shown in Figure 3, which are used to control and monitor high fidelity simulations and equipment such as the Real-Time Digital Simulator shown in Figure 4.

Figure 3: Two phasor measurement units from the TCIPG testbed at University of Illinois Urbana-Champaign.

Figure 4: Real-Time Digital Simulator

Contents of this paper

For the remainder of this paper, we will first discuss the structure of the P.I.A. vector tracking loop and our approach to implementing the tracking loop. Section "Experimental Setup" discusses the equipment and location used in performing the field experiment. Section "Test Results" presents the performance of the P.I.A.

vector tracking loop as well as the results from a meaconing attack simulation.

STRUCTURE

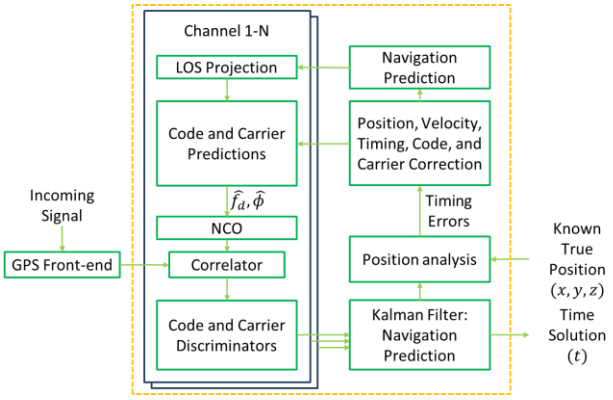

Figure 5: Position-Information-Aided Tracking Loop

The structure of the P.I.A. vector tracking loop is shown in Figure 5. In P.I.A. vector tracking, information from the navigation filter and the known true position is fed back into the tracking loop and used to control the numerically controlled oscillator (NCO). As a result the channels share information with one another and are able to aid channels with weak signal-to-noise ratios through the use of a common static receiver's position, velocity, and clock bias.

In comparison to our P.I.A. vector tracking approach, traditional scalar tracking processes each channel independently, and there is no feedback of information between the navigation filter and the tracking loops. As such, scalar tracking neglects to take into account the relations between satellites and the user position and velocity. By leveraging this information in our P.I.A. vector tracking algorithm, the search space is narrowed considerably in the (x, y, z) dimensions.

In implementing the position-information-aided vector tracking algorithm, we actively drew on the previous vector tracking research completed by Zhao and Akos [10] as well as the open source MATLAB SDR code created by Borre and Zhao [11]. The open source vector tracking code designed by Zhao and Akos was designed to operate under high dynamics and low signal-to-noise environments. For the purposes of implementing the P.I.A. vector tracking, we have extensively modified the existing vector tracking code for operation under no dynamics and low signal-to-noise situations.

Overall flow

P.I.A. vector tracking loops are meant to be used in conjunction with the existing scalar loops. At a specific time epoch the following are extracted from the scalar tracking results and used to initialize the P.I.A. vector tracking loop: code phase ($\varphi_{j,k}$), code frequency ($f_{code,j,k}$), carrier frequency ($f_{j,k}$), signal transmit time ($t_{trans,j,k}$), clock bias ($t_{b,k}$), and clock drift ($t_{d,k}$). Where the subscripts j represents the jth satellite and k represents the kth epoch. Since the P.I.A. vector tracking is loosely dependent on these initial values, we choose to initialize our tracking loop after the scalar loop has gained a strong fix on the signal.

After initialization, the P.I.A. vector tracking loop first predicts the navigation solution and errors for the next time epoch. Then early, late, and prompt code replicas are generated using the LOS projections to calculate the predicted Doppler and phase terms. The code replicas are then used to create correlations with the signal from the GPS front end which is then used generate the code and carrier discriminators. The discriminators from each channel contain the code and carrier errors which is then projected onto the LOS vectors and used to generate the Kalman filter measurement matrix. The Kalman filter then estimates the new errors and based on the updated errors we can estimate the new navigation solution and create a prediction for the next time epoch. Since we know the true position of the GPS receiver, we then correct the prediction and create a closed feedback loop using the corrected predictions.

Detailed flow

The process for the P.I.A. vector tracking algorithm can be broken down into 4 main groups: 1. Estimation of the NCO parameters, 2. Discriminator calculation and processing, 3. Navigation error estimation and navigation prediction, 4. Navigation correction and error correction using the true position and feedback. In the next section, we will go over each of these groups in greater detail.

1. Estimation of the NCO parameters.
The NCO uses carrier frequency and phase estimates to generate code replicas used for correlation. Since the carrier frequency and phase terms are directly influenced by the geometry and movement of the satellites with respect to the PMU GPS receiver, we simply need to use the satellite positions and velocities to estimate these terms.

We assume that the ephemeris values are known from either scalar tracking results or external sources. Then the satellite positions from the kth epoch can be generated and the satellite positions and velocities are then used to estimate the pseudorange, the LOS unit vector, and find the relative velocity between the satellite and the PMU receiver. The code phase and carrier frequencies can then be calculated based on the previous estimated terms. The true position of the receiver is assumed to be known and therefore the predicted position and velocity is given by the following equations.

$$\hat{X}_{k+1} = X_{true} \quad (1)$$

$$\hat{V}_{k+1} = V_{true} \quad (2)$$

Where X_{true} is the PMU receiver position and V_{true} is the PMU receiver velocity. We denote position and velocity predictions for the next time epoch as $\hat{X}_{k+1}$ and $\hat{V}_{k+1}$. Once the position and velocity projections are calculated the code phase/frequency, carrier frequency, and clock drift prediction equations are given in equations 5-8 of Zhao and Akos [10].

From the estimated code phase and carrier frequencies, replicas of the code are generated and used to create correlations with the received GPS signal at the corresponding time epoch.

2. Discriminator calculation and processing.

The NCO generates early, prompt, and late replicas which are used to create correlations with the incoming signals. We will denote the inphase early, prompt, and late correlations as I_E, I_P, and I_L. Similarly, quadrature correlations will be denoted as Q_E, Q_P, and Q_L.

In this work, we chose to only use carrier frequency discriminators since carrier phase tracking is not suited for low signal-to-noise environments, as is the case during interference or jamming attacks.

For the code phase discriminator, we chose to use:

$$\frac{1}{2}\frac{E-L}{E+L}$$

where $E = \sqrt{I_E^2 + Q_E^2}$ and $L = \sqrt{I_L^2 + Q_L^2}$. This discriminator, described in [12], is a noncoherent early minus late envelope normalized by $E + L$ to remove amplitude sensitivity.

We chose to use a normalized decision directed frequency discriminator as described in table 5.4 of [12]:

$$\frac{(cross) \times sign(dot)}{2\pi(t_2 - t_1)(I_{P2}^2 + Q_{P2}^2)}$$

where $cross = I_{P1}Q_{P2} - I_{P2}Q_{P2}$, $dot = I_{P1}I_{P2} - Q_{P1}Q_{P2}$, and the $P1$ and $P2$ subscripts represent the results over current epoch and the previous epoch. The discriminator outputs are then used to generate the Kalman filter measurement matrix.

3. Navigation error estimation and navigation prediction.

The discriminators output the code phase errors and carrier frequency errors which contain the corresponding LOS projections of the errors between the estimated position and velocity and the known true position and velocity. The relationship between the code phase error and carrier frequency errors with the user position error can be modeled as:

$$e_{code,k} = \hat{\varphi}_{j,k} - \varphi_{j,k} \quad (3)$$

$$e_{carr,k} = f_{j,k} - \hat{f}_{j,k} \quad (4)$$

where e_{code} and φ are in meters, and e_{carr}, and f are in meters/sec. By using the calculated LOS projections ($a_{j,k}$), we can rewrite (3) and (4) as functions of the clock bias and change in clock drift:

$$e_{code,k} = t_{b,k} + \left(X_k - \hat{X}_k\right)^T a_{j,k} \quad (5)$$

$$e_{carr,k} = \Delta t_{d,k} + \left(V_k - \hat{V}_k\right)^T a_{j,k} \quad (6)$$

The position and velocity errors can be modeled as the difference between the true PMU receiver position and the calculated position and velocity:

$$\delta X_k = X_{true} - X_k \quad (7)$$

$$\delta V_k = V_{true} - V_k \quad (8)$$

In each of the equations above, there is an implied error term that has not been included.

We can see from the error analysis, if the position and velocity errors can be estimated, the navigation solution can also be calculated. Therefore in implementing the P.I.A. vector tracking, we chose the position errors, velocity errors, clock bias error, and clock drift error as the states of the Kalman filter. Since we know the initial position, velocity, clock bias, and clock drift values from the scalar tracking results, the navigation solution can be estimated through the errors.

Then $\delta X, \delta V, \delta t_b$, and δt_d are the states of our system and the discrete process equation is given by

$$\begin{bmatrix} \delta X_{k+1} \\ \delta V_{k+1} \\ \delta t_{b,k+1} \\ \delta t_{d,k+1} \end{bmatrix} = F_{k,k+1} \begin{bmatrix} \delta X_k \\ \delta V_k \\ \delta t_{b,k} \\ \delta t_{d,k} \end{bmatrix} \quad (9)$$

where,

$$F_{k,k+1} = \begin{bmatrix} 0 & \Delta t & 0 & 0 \\ 0 & 0 & 0 & 0 \\ 0 & 0 & 0 & \Delta t \\ 0 & 0 & 0 & 0 \end{bmatrix}$$

where Δt is given by the time difference between the kth and $(k+1)$ time epoch. The Kalman Filter measurement equation is then given in equation 10 of Zhao and Akos [10]:

$$Z_k = HX_k + V_k$$
$$= \left[z_{code,1,k}\ z_{carrier,1,k}\ \cdots\ z_{code,n,k}\ z_{carrier,n,k}\right]^T_{1x2n}$$

where the terms of the H matrix are determined by the following equations:

$$z_{code,j,k} = a_{j,k}\delta X + t_{b,k}$$
$$z_{carrier,j,k} = a_{j,k}\delta V + \Delta t_{d,k}$$

where $\Delta t_{d,k}$ is the change in the clock drift error.

Since the states of the Kalman filter were chosen to be error of the position, velocity, clock bias, and clock drift, we can then correct our predictions as:

$$X_{k+1} = \hat{X}_{k+1} + \delta X_{k+1} = X_{true} + \delta X_{k+1} \quad (10)$$

$$V_{k+1} = \hat{V}_{k+1} + \delta V_{k+1} = V_{true} + \delta V_{k+1} \quad (11)$$

$$t_{d,k+1} = \hat{t}_{d,k+1} + \delta t_{d,k+1} \quad (12)$$

$$t_{b,k+1} = \hat{t}_{b,k+1} + \delta t_{b,k+1} \quad (13)$$

where the 'hat' indicates the predictions from the previous time epoch. The corrected predictions shown here are then output as our navigation solutions.

In the P.I.A. vector tracking loop, the bandwidth is controlled by the Kalman filter which makes it difficult to pinpoint the exact bandwidth that is being used as the adaptive Kalman filter gain, K, is proportional to the bandwidth. Thus, in this work, the bandwidth was set empirically by controlling the Kalman filter Q and R matrices which represent the uncertainty in the dynamics of the user and the noise in the discriminator outputs. More detailed explanations can be found in [10]. However, to compare the scalar and P.I.A. vector tracking results the tracking loop bandwidths should be relatively similar. Therefore, we empirically adjusted the Q and R matrices such that the basic vector tracking loop's performance closely matched that of the scalar tracking loop using a 5Hz bandwidth, due to the receiver being static, and used the same Q and R values in our P.I.A vector tracking loop.

4. Navigation correction and error correction using the true position and feedback.
Once the position and velocity predictions have corrected by the Kalman filter, we then compare the corrected predictions with our known true position and velocity. By taking into account the true position, we can estimate the errors for the next time epoch using (7) and (8) and feedback the predicted errors back into the tracking loop to form a closed loop.

Then the code frequency, code phase, and carrier frequency can be corrected as:

$$f_{code,j,k+1} = \hat{f}_{code,j,k+1} + \left(t_{d,k+1} + \delta \mathrm{V}_{k+1} a_{j,k}\right) * f_{code}/c \quad (14)$$

$$\varphi_{j,k+1} = \hat{\varphi}_{j,k+1} + \delta X_{k+1}^{T} a_{j,k} + c\Delta t + t_{b,k} \quad (15)$$

$$f_{carrier,j,k+1} = \hat{f}_{carrier,j,k+1} + \left(t_{d,k+1} + \delta \mathrm{V}_{k+1} a_{j,k}\right) f_{carrier}/c \quad (16)$$

5. Calculating GPS receiver clock bias.
Since we know the true position of the receiver, we can accurately calculate the clock bias of the receiver as a weighted average of the difference between the calculated pseudorange and actual range. Equation 4.7 from Heng [13]:

$$t_b = \frac{1}{\sum_{j=1}^{J} \omega_j} \sum_{j=1}^{J} \omega_j (\tilde{\rho}^{(j)} - \left| x^{(j)} - x \right|)$$

where $\omega_j = 1/var(\epsilon)$, $\tilde{\rho}^{(j)}$ is the calculated pseudorange between the PMU receiver and the jth satellite, $x^{(j)}$ is the position of the jth satellite, and x is the known true position.

EXPERIMENTAL SETUP

We conducted field experiments to determine the performance of the P.I.A. vector tracking algorithm compared with the traditional tracking algorithm. We use off-the-shelf low-cost SiGe GN3S GPS sampler as the front-end to collect raw GPS signals.

The SiGe front-end is a thumb-sized USB device designed to operate in conjunction with a software-defined receiver (SDR) as shown in Figure 6. It uses a sampling frequency from 4 MHz to 16 MHz and a quantization resolution of 2 bits. Since the quality of the GPS receivers used in PMUs are generally higher than that of a SiGe sampler, the results we obtain using data collected using the low-cost SiGe will provide a conservative lower-bound estimate of results collected using PMU receivers.

For this experiment we used a fixed-reference choke ring antenna in conjunction with the SiGe sampler. During data collection the antenna had full view of an open sky with up to 10 satellites with clear LOS. The data was then post-processed using the software-defined-receiver (SDR) for both scalar and P.I.A. vector tracking.

Figure 6: Low cost receiver - SiGe sampler.

Figure 7: Fixed reference antenna with full access to the open sky.

TEST RESULTS

In this section, we will discuss the performance of the P.I.A. vector tracking algorithm. After processing the collected data, the acquisition module of our SDR was able to acquire 9 of the 10 satellites in view. Then then data was processed using first the scalar tracking loop and navigation module. Then the scalar tracking results were then used to initialize the P.I.A. vector tracking loop.

When compared with scalar tracking results, the P.I.A. vector tracking loop is expected to more accurately predict the code and carrier frequencies needed to track the signal, and as a result we obtain more accurate PVT solutions. Results over a 50 second time span are shown in figures 7-16. Figures 8-10 show the code frequency difference from the GPS code frequency (1.023e6) and Figures 11-13 show the Doppler frequencies for the first 3 channels. From the figures, we can see that the code and carrier frequencies calculated in the P.I.A. vector tracking loop are more accurate and precise than the frequencies from the scalar counterparts.

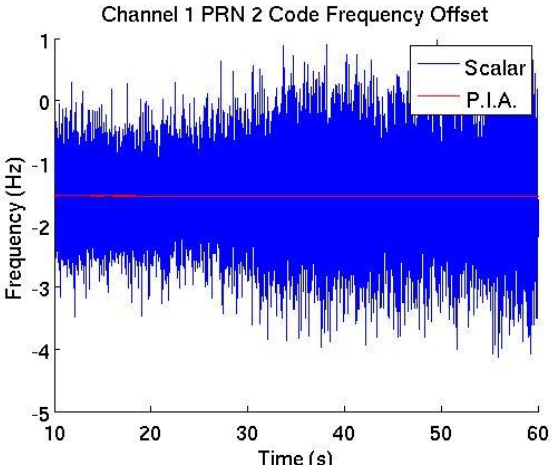

Figure 8: Code frequency results from PRN 2

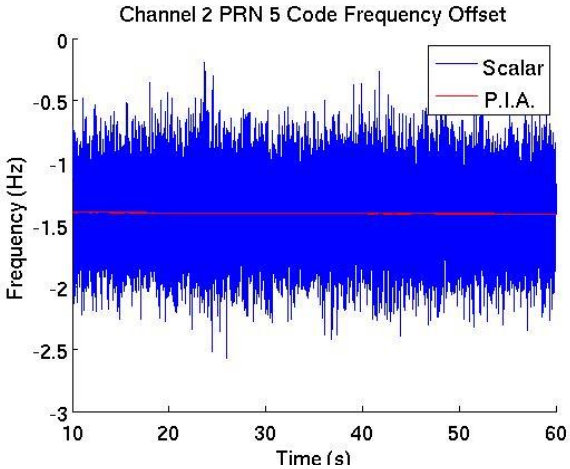

Figure 9: Code frequency results from PRN 5

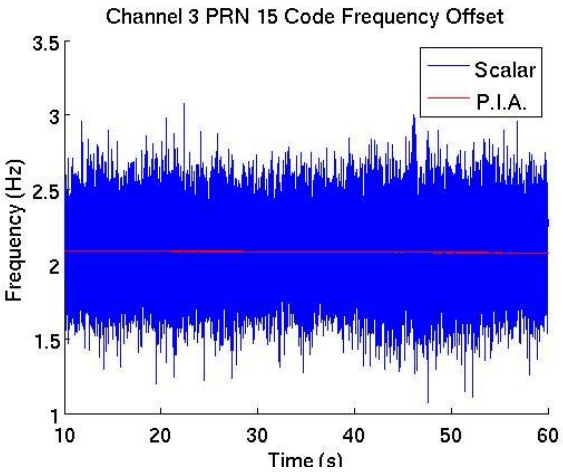

Figure 10: Code frequency results from PRN 10

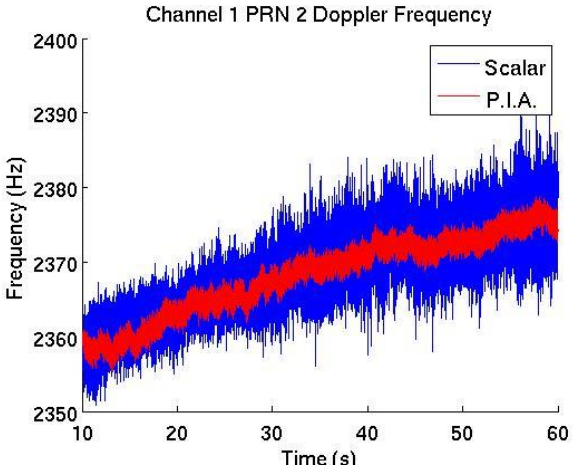

Figure 11: Doppler frequency results from PRN 2

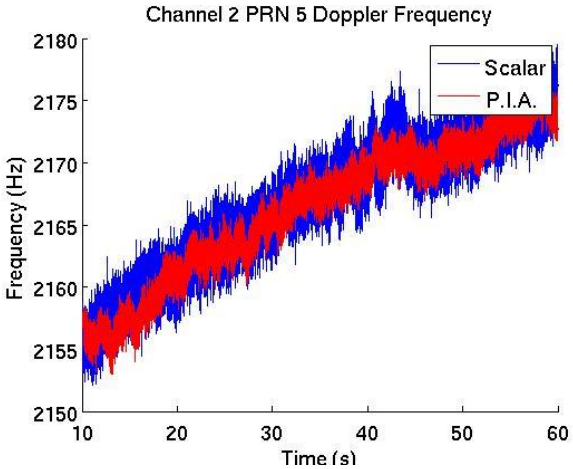

Figure 12: Doppler frequency results from PRN 5

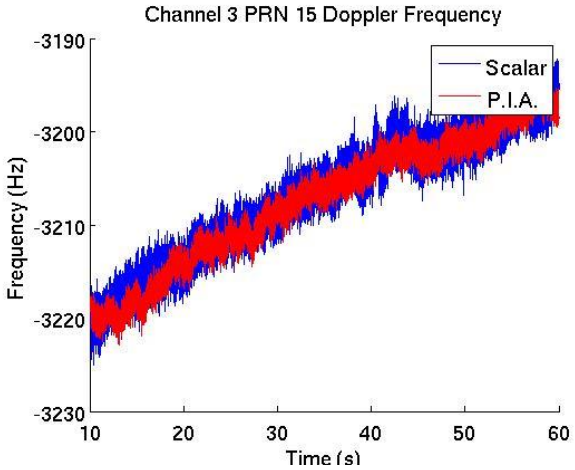

Figure 13: Doppler frequency results from PRN 10

Noise tolerance performance

To determine the performance of the P.I.A. vector tracking algorithm, we added 1-10 dB of simulated Gaussian noise to the raw GPS signal and processed the resulting data. Figures 14-16 show the time error results for varying levels of added noise. With no added noise, the maximum time errors for the scalar results were close to 45 ns whereas the time errors for the P.I.A. results were around 10 ns.

Scalar tracking was able to produce decodable navigation bits up until we increased the noise past 4dB. However, with every dB of additional noise, the number of channels that experienced a loss-of-lock increased. At 4 dB of additional noise, the scalar tracking loop was only able to lock onto 4 satellites while the original data could lock onto all 9. The time errors also increased as the noise increased: scalar results showed close to 60 ns of maximum errors and P.I.A. results showed maximum errors of 13 ns.

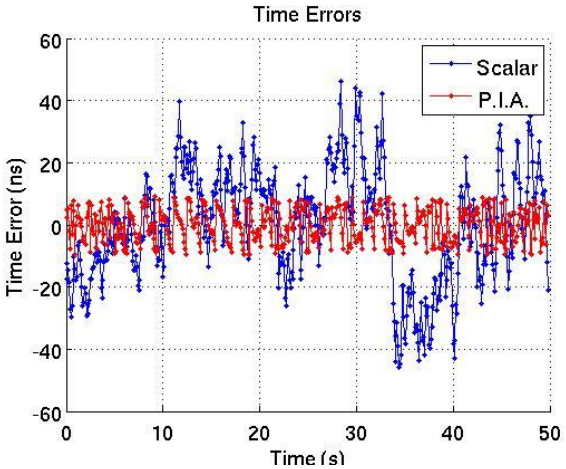

Figure 14: Time errors with no added noise

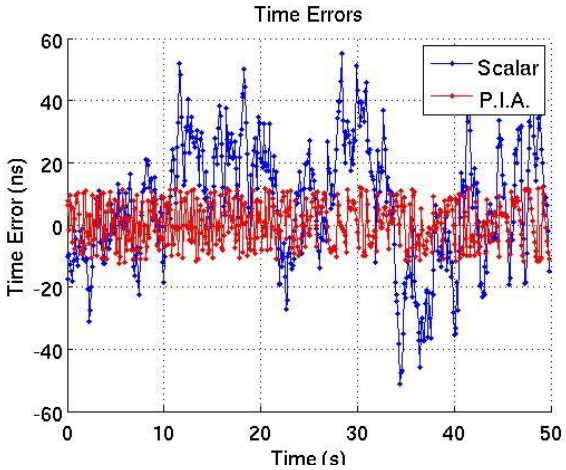

Figure 15: Time errors with 4 dB of added noise

The P.I.A. vector tracking loop continued operating until we increased the noise past 9dB, at which point the maximum time errors were close to 20 ns.

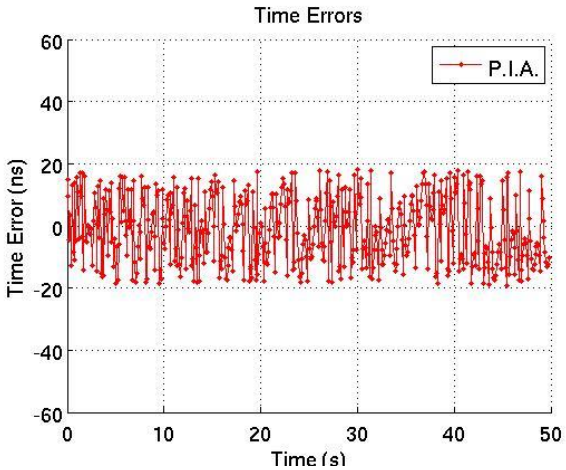

Figure 16: Time errors with 9 dB of added noise. Scalar tracking has stopped working.

Meaconing attack simulation

The P.I.A. vector tracking algorithm is designed to function with the known true position as the reference point. In a meaconing attack, also known as the record-and-replay attack, the GPS signal is first received by the attacker and then broadcast at a higher signal-to-noise ratio than the signals received from the satellites, causing the GPS receivers to lock onto the meaconed signal. A traditional scalar tracking loop would continue to operate during a meaconing attack, However the PVT solution calculated would be equal to PVT solution of the attacker, plus a delay, thus provides wrong and misleading timing information. Figure 16 shows the results of a meaconing attack simulation. Due to the fixed-position nature of the P.I.A. vector tracking loop, the algorithm fails to converge as soon as the meaconing attack begins. Therefore, our

proposed P.I.A vector tracking is able to successfully detect meaconing attack.

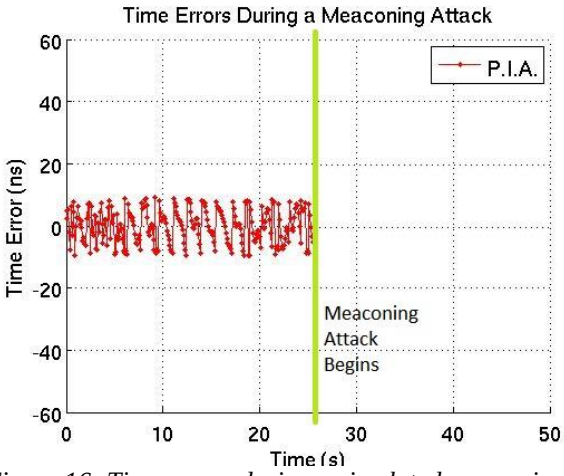

Figure 16: Time errors during a simulated meaconing attack with a 200m separation between the spoofer and the PMU GPS receiver.

CONCLUSION

Since PMUs are reliant on clock readings from the GPS system, the reliability and security of the GPS receiver is crucial. In this paper, we investigated position-information-aided vector tracking loop to improve the robustness of GPS receivers used in PMUs against jamming and spoofing attacks. We have discussed the underlying concept, modeled and implemented the proposed tracking loop in a software-defined-receiver, and conducted field experiments to evaluate the performance of the algorithm.

The field experiments showed that by utilizing the static nature of the GPS receivers used in PMUs, we are able to reduce the search space of the vector tracking loop and improve the accuracy of time solutions generated by the static receiver. We have demonstrated improved robustness against noise and jamming, as well as the ability to successfully detect meaconing attacks.

ACKNOWLEDGMENTS

This material is based upon work supported by the Department of Energy under Award Number DE-OE0000097.

REFERENCES

[1] U.S. Energy Information Administration, “Today in Energy”, Retrieved from: http://www.eia.gov/todayinenergy/detail.cfm?id=5630

[2] Warburton, J., and C. Tedeschi, “GPS Privacy Jammers and RFI at Newark: Navigation Team AJP-652Results,”12th International GBAS Working Group Meeting (I-GWG-12), Atlantic City, New Jersey, November 17, 2011.

[3] Tedeschi, C., “The Newark Liberty International Airport (EWR) GBAS Experience,” 12th Inter- national GBAS Working Group Meeting (I-GWG- 12), Atlantic City, New Jersey, November 17, 2011.

[4] T. E. Humphreys, B. M. Ledvina, M. L. Psiaki, B. W. O’Hanlon, and J. Kintner, Paul M., “Assessing the spoofing threat: Development of a portable GPS civilian spoofer,” in Proceedings of the 21st International Technical Meeting of the Satellite Division of the Institute of Navigation (ION GNSS 2008), Savannah, GA, Sep. 2008, pp. 2314–2325.

[5] X. Jiang, J. Zhang, B. J. Harding, J. J. Makela, and A. D. Domínguez-García, “Spoofing GPS receiver clock offset of phasor measurement units,” IEEE Transactions on Power Systems, vol. 28, no. 3, pp. 3253–3262, 2013.

[6] J. S. Warner and R. G. Johnston, “A simple demonstration that the Global Positioning System (GPS) is vulnerable to spoofing,” Journal of Security Administration, vol. 25, no. 2, pp. 19–27, 2002.

[7] GPS.gov, “GPS Spectrum and Interference Issues”, Retrieved from: http://www.gps.gov/spectrum/

[8] Federal Communications Commission, Deere submission: LightSquared Interference to GPS and StarFire, May 26, 2011

[9] L. Heng, J. J. Makela, A. D. Dominguez-Garcia, R. B. Bobba, W. H. Sanders, and G. X. Gao, “Reliable GPS-Based Timing for Power Systems: A Multi-Layered Multi-Receiver Architecture,” IEEE PECI 2014, Champaign, IL, Feb 2014

[10] Zhao and Akos, "An Open Source GPS/GNSS Vector Tracking Loop – Implementation, Filter Tuning, and Results", International Technical Meeting of the Institute of Navigation, San Diego, CA, January 2011, pp. 1293-1305.

[11] K. Borre, D. M. Akos, et al. "A Software-Defined GPS and Galileo Receiver: A Single-Frequency Approach", Springer, New York, 2007

[12] E. D. Kaplan, C. J. Hegarty, "Understanding GPS: Principles and Applications, 2nd Ed", Artech House Inc, MA, 2006

[13] L. Heng, 2012, "Safe Satellite Navigation with Multiple Constellations: Global Monitoring of GPS and Glonass Signals-In-Space Anomalies", Ph.D., Stanford, USA